Multi-UAV Cooperative Decision-Making under Noisy and Uncertain Environments

***Abstract*—In the process of multi-UAV cooperative decision-making, the information evolution model plays a key role in the communication and fusion of information among multiple agents. However, traditional information fusion models, such as the DeGroot model and the Hegselmann-Krause bounded confidence (HK) model in opinion dynamics, have certain limitations in handling complex noisy environments, adjusting weights dynamically, and processing linguistic information. To address these challenges, this paper proposes an information fusion model that integrates the social network mechanism, the hyperbolic tangent function, and the Monte Carlo method. In each round of information iteration, the model uses the social network structure to simulate the communication relationships among agents. Specifically, the social network is represented as a binary adjacency matrix. Then, a distance measure between linguistic information is defined. Based on this distance, the hyperbolic tangent function is used to determine the weights of agents during the evolution process dynamically. To fully evaluate the model's performance under noise, Monte Carlo simulations are used for statistical analysis. A case of multi-UAV cooperative reconnaissance is presented to validate the effectiveness of the model. In addition, detailed comparisons with several existing models are conducted. The experimental results show that the proposed model demonstrates clear advantages in terms of anti-interference capability, stability, and adaptability to various linguistic information environments.**

***Note to Practitioners*—This paper presents an information fusion model in multi-UAV cooperative decision-making. Traditional opinion dynamics models often struggle with noisy environments, fixed weighting, and complex linguistic information. To address these issues, the proposed model integrates social network structures, a hyperbolic tangent-based weighting mechanism, and Monte Carlo simulations for robustness evaluation. It supports dynamic information adjustment and is well-suited for uncertain scenarios. A case study on UAV cooperative reconnaissance demonstrates the model's practical value in enhancing stability, adaptability, and resistance to interference in real-world multi-agent systems.**

***Index Terms*—Opinion Dynamics, Social Network, Linguistic Information.**

I. Introduction

CURRENTLY, UAVs are widely used in various fields, including military reconnaissance [1], emergency rescue [2], [3], and industrial inspection [4], [5]. As technology advances, the complexity of UAV tasks continues to grow, especially for UAV swarms. In typical post-disaster scenarios, such as earthquakes, affected areas are often difficult to access manually due to collapsed buildings, blocked roads, or ongoing risks of secondary disasters. In such situations, deploying multiple UAVs provides a fast and flexible way to perform aerial inspections over large regions. In this context, multi-UAV cooperative decision-making mainly involves sharing local information among UAVs, assessing the level of local damage, and reaching a collective understanding of the overall disaster situation through information fusion. When multiple UAVs carry out missions, the key is to integrate the information from each UAV to develop a comprehensive situational awareness and make optimal decisions [6]. At present, the main approaches are summarized as follows.

Each UAV sends its information to a central node, which then plans the entire system. Once the optimal decisions are calculated, the central node distributes them to each UAV for execution. Usually, the centralized decision-making is regarded as an optimization problem. For example, the multi-agent decision-making optimization was studied under a fuzzy uncertain environment and centralized decision-making mode, which focused on equilibrium and compensation of multi-agent problems in [7]. Although optimization methods can solve most centralized decision-making problems, they rely heavily on the central node. If the central node fails, the entire system may stop working.

Compared to centralized decision-making, collaborative decision-making operates without the need for a central node. In this method, each UAV is an independent computing and analysis unit, making decisions by exchanging information with other UAVs. For example, a distributed adaptive algorithm based on individual decision-making and group decision-making was proposed in [8]. In [9], the soft actor critic (SAC) algorithm was extended to the multi-agent domain and embed with the graph attention neural network into the actor, critic network. A broad discussion on game-theoretic approaches in multi-agent systems, covering cooperative and non-cooperative scenarios, was proposed in [10]. In [11], the authors suggested a self-optimization model integrating cellular automata and game theory, simulating competitive evolutionary interactions among agents. Also, a three-strategy decision model, where agents adopted conservative and adaptive strategies based on their interactions with neighbors, was proposed [12]. Apart from the above methods, the opinion dynamics model, as a method capable of handling uncertainty, has attracted increasing attention in recent years. It enables intelligent agents to express their understanding using linguistic terms and to reach group consensus through continuous opinion updating. This makes it especially suitable for multi-UAV collaborative tasks where sensor perceptions are diverse and the available information is uncertain or vague [13]–[16]. In [17], a self-confidence evolution model, which encompassed the self-confidence levels of one's group mates and the passage of time, was proposed. Besides, a novel group decision-making (GDM) model with information evolution was established, and a consensus model with minimum adjustments was provided to obtain the optimal adjusted initial information and collective consensus results [18]. An information similarity mixed model and a structural similarity mixed (SSM) model were proposed in [19], in which the strong and weak relations between agents were considered, and the network was dynamically updated based on information similarity and structural similarity. In [20], a value function-based consensus model was developed, identifying a consensus ranking by considering ordinal and cardinal information within subgroups. In [21], a personalized individual semantics (PISs)-based individual consensus-level maximization model and a PIS-based minimum adjustment model were established for consensus reaching in linguistic group decision making (GDM). In [22], a conflict resolution method considering the trust propagation, conflict detection and elimination, and alternative selection was proposed. For the model in [23], the agents updated their beliefs by taking a weighted average of their information and the information of their neighbors in a network. In [24], [25], each agent considered only the information of others within a predefined confidence interval around its own and updated its information by averaging this selected information.

In addition, linguistic expressions play an important role in many real-world applications. On one hand, they reflect the natural way people describe situations in everyday life. On the other hand, in many scenarios, the information is often uncertain and incomplete. In such cases, linguistic expressions offer a practical and flexible way to represent uncertainty. For example, the propagation of distributed linguistic trust was investigated to study the trust relationships among experts, and a new feedback mechanism was proposed for social network group decision making (SN-GDM) in [26]. In [27], a novel consensus-based linguistic distribution large-scale group decision-making (CLDLSGDM) approach based on a statistical inference principle that considered DMs' regret aversion psychological characteristics was proposed. Also, the comparative linguistic expression and three-way decision were combined to form a new multiattribute three-way group decision-making (3WGDM) method in [28]. To deal with the group-making problems with multigranular unbalanced hesitant linguistic information, the authors in [29] proposed an algorithm to represent a linguistic distribution assessment (LDA) using a hesitant linguistic distribution (HLD).

After reviewing the relevant literature, it becomes clear that the linguistic expression provides a flexible and intuitive way to express the uncertainty in complex environments [28]. However, many existing studies on opinion dynamics still rely heavily on precise numerical representations. In such cases, it is not easy to fully describe the complexity of the situation using only precise numerical data. Additionally, the traditional models have some limitations. For example, the Hegselmann-Krause bounded confidence (HK) model, which is widely used in opinion dynamics, has two main limitations [23]–[25]. First, it is susceptible to the confidence threshold value. Even a slight difference in this value can lead to completely different results. Second, determining the most appropriate or accurate confidence threshold remains a challenging task. This is mainly because different application scenarios often require different standards for setting the threshold. Moreover, in some extended versions of the model, each agent may have its confidence threshold, which further increases the subjectivity and complexity of the decision-making process. Furthermore, in many past studies related to decision-making, the impact of noise interference was often overlooked. However, in real-world applications, especially in multi-UAV collaborative decision-making scenarios, noise is an unavoidable and important factor. For example, during collaborative decision-making tasks, UAVs need to share information. In such situations, communication systems may face various types of noise, such as signal loss, multipath effects, or sudden disruptions. These types of interference can directly affect the quality of the information each UAV receives. If such noise is not modeled correctly and managed, it can reduce the accuracy of individual UAV decisions and affect the final results.

Motivated by the above challenges, this paper proposes an improved information fusion model for multi-UAV cooperative decision-making. The theoretical contributions and advantages of this study can be summarized as follows: (1) a social network mechanism is incorporated into the opinion dynamics framework to capture the interaction structure among UAVs realistically; (2) a hyperbolic tangent function is introduced to adaptively determine interaction weights based on the divergence of linguistic information, improving stability; (3) Monte Carlo simulations are integrated to explicitly model noise and randomness, enabling robust evaluation under uncertain conditions; and (4) this paper integrates opinion dynamics with multi-UAV cooperative decision-making. Based on this integration, we establish a complete framework that provides a new approach to addressing cooperative decision-making problems of UAV swarms in practical scenarios such as disaster response.

The paper's structure is as follows: In Section II, the relevant concepts are introduced. In Section III, the new model is proposed. In Section IV, a series of examples are presented. In Section V, the comparison and robustness analysis are conducted. The conclusion is given in Section VI.

II. Preliminaries

A. DeGroot Model

Definition 1 [23]: Suppose that $E = \{e_1, e_2, \cdots, e_N\}$ represents the agents. $t \in \{1, 2, \cdots, T\}$ indicates the number of rounds of opinion evolution. $\upsilon_n(t)$ is the opinion of e_n at time t. The weight of e_j in e_i's opinion update process is ω_{ij}, where $0 \leq \omega_{ij} \leq 1$ and $\sum_{j=1}^{N} \omega_{ij} = 1$ for all $i \in N$. The opinion evolution rule is:

$$\upsilon_i(t+1) = \sum_{j=1}^{N} \omega_{ij} \upsilon_j(t). \tag{1}$$

B. HK Bounded Confidence Model

Definition 2 [24], [25]: Following the notation in *Definition 1*, let ε indicate the confidence threshold value. If all agents hold the same confidence threshold ε, the HK model is homogeneous; otherwise, it is heterogeneous.

Step 1: Determine the confidence set.

Let $I(e_i, X(t))$ be the confidence set of e_i at time t.

$$I(e_i, X(t)) = \{e_j \,|\, |\upsilon_i(t) - \upsilon_j(t)| \leq \varepsilon, e_j \in E\}. \tag{2}$$

Step 2: Calculate the weights.

When the agent e_i update the opinion at time t, the weight of the agent e_j is:

$$\omega_{ij}(t)=\begin{cases}\frac{1}{\#I(e_i,X(t))}, & \text{if } e_j\in I(e_i,X(t))\\ 0, & \text{otherwise}\end{cases} \tag{3}$$

where $\#I(e_i,X(t))$ is the cardinality of $I(e_i,X(t))$.

Step 3: Opinion evolution.

Let $\upsilon_i(t+1)$ indicates the opinion of e_i at time $t+1$, then

$$\upsilon_i(t+1)=\omega_{i1}\upsilon_1(t)+\omega_{i2}\upsilon_2(t)+\cdots+\omega_{iN}\upsilon_N(t) \tag{4}$$

C. Linguistic Term Set

Definition 3: Let $S=\{s_0,s_1,\cdots,s_{2\Phi},|\Phi\in N^*\}$ be a finite and completely ordered linguistic term set (LTS). s_i represents a possible value for a linguistic variable. s_i and s_j should satisfy [30], [31]:

(1) $s_i\le s_j$ if and only if $i\le j$;
(2) The negation operation $neg(s_i)=s_j$ if $i+j=2\Phi$;
(3) If $i\ge j$, then $\max\{s_i,s_j\}=s_i$;
(4) If $i\ge j$, then $\min\{s_i,s_j\}=s_j$.

D. Linguistic Scale Functions (LSFs)

Definition 4: For the linguistic term h_ξ in $H=\{h_\xi|\xi=0,1,\cdots,2\Phi,|\Phi\in N^*\}$, h_ξ represents a possible value for a linguistic variable. If $\theta\in[0,1]$ is a numerical value, then the function $f:h_\xi\to\theta_\xi$, which conducts the mapping from h_ξ to θ_ξ ($\xi=0,1,\cdots,2\Phi$), is defined as follows:

$$\theta_\xi=\begin{cases}\frac{a^\Phi-a^{\Phi-\xi}}{2a^\Phi-2}, & 0\le\xi\le\Phi\\ \frac{a^\Phi+a^{\xi-\Phi}-2}{2a^\Phi-2}, & \Phi<\xi\le2\Phi\end{cases} \tag{5}$$

where $\theta_\xi\in[0,1]$. The maximum value of θ_ξ is 1, obtained when ξ is 2Φ, and the minimum value is 0, obtained when ξ is 0. [32] states that a is most likely to belong to the interval of $[1.36,1.4]$ through a mess of experiments.

E. Social Network

Definition 5 [33]–[36]: A social network is $G(V,E)$. $V=\{v_t,\ t\in M\}$ expresses vertices. $E=\{e_{ts},\ t,s\in M\}$ indicates the edges. The edge $e_{ts}=(v_t,v_s)$ indicates the relationship between v_t and v_s. $F=(f_{ts})_{m\times m}$ can describe the social network.

$$f_{ts}=\begin{cases}1, & (v_t,v_s)\in E\\ 0, & otherwise\end{cases} \tag{6}$$

Definition 6 [37], [38]: For $G(V,E)$, the following concepts are introduced.

Density of social network:

It is the ratio of the number of direct pairwise relationships to the possible number of direct relationships.

In-degree $C_{id}(v_t)$ of the vertex v_t:

It is employed to describe the reputation of a node, which reflects the integration force.

Out-degree $C_{od}(v_t)$ of the vertex v_t:

It is used to describe the communicative nature of a node, which reflects the radiation.

III. Problem Description and Model Proposal

In natural disasters, military reconnaissance, and environmental monitoring, quickly and accurately obtaining real-time information about a target area is crucial for making decisions. However, traditional reconnaissance methods rely mainly on ground surveys, satellite remote sensing, and manned aerial photography. These methods are often limited by weather conditions, terrain, and communication environments, resulting in slow data acquisition, limited coverage, and delayed information updates. In recent years, with the development of multi-UAV cooperative technology, UAV swarm intelligence systems have demonstrated a high level of autonomy and efficient information-sharing capabilities across various fields. It is worth noting that this study is inspired by the research presented in [39]. As shown in Fig. 1, a group of n UAVs is cooperatively circumnavigating a group of m unknown targets on a horizontal plane, and taking post-earthquake rescue in mountainous areas as an example. Multiple UAVs are deployed to conduct reconnaissance flights around a key post-earthquake area. The goal is to collect information about the structural stability and potential collapse risks of the area. However, due to differences in flight altitude, observation angle, sensor accuracy, and other factors, the quality and focus of the data collected by each UAV may vary. As a result, even when observing the same area, the risk assessments provided by different drones may differ. For example, a UAV flying at a low altitude with a high-resolution camera may detect visible cracks and classify the area as "high risk." In contrast, another drone flying at a higher altitude with lower image clarity may classify the same area as "medium risk." To address the judgment differences caused by such variations in perception, this paper introduces the opinion dynamics model. Each drone treats its local linguistic risk assessment as an opinion. Through multiple rounds of communication with other UAVs, each UAV updates its evaluation by integrating the information received from others. This process allows the system to gradually reach a consistent and reliable assessment of the risk level in the target area at the collective level. The final risk evaluation, such as classifying a region as "high risk" or "low risk", provides a basis for rescue decision-making. It helps the command center determine whether rescue forces should be deployed immediately and decide on the type and amount of resources to send, such as human rescue teams or reconnaissance robots.

Step 1: Initialization

Suppose that $E=\{e_1,e_2,\cdots,e_N\}$ indicates the agents, and the LTS is $H=\{h_\xi|\xi=0,1,\cdots,2\Phi,|\Phi\in N^*\}$. $t\in\{0,1,\cdots,T\}$ indicates the discrete variable representing the number of rounds of information evolution. $\Upsilon_n(t)$ is the linguistic information of e_n at time t, and $\upsilon_n(t)$ is the corresponding numeric value of $\Upsilon_n(t)$. The weight of e_j in e_i's information update process is ω_{ij}, where $0\le\omega_{ij}\le1$ and $\sum_{j=1}^{N}\omega_{ij}=1$ for all $i\in N$. In the process of information updating, the noise interference $X\sim\mathcal{N}(\mu,\delta^2)$ is assumed to follow the normal distribution, with both its mean μ and standard deviation δ varying across different update iterations.

Step 2: Transform Linguistic Terms into Numerical Values

After obtaining the linguistic term h_ξ, the next step is to convert it into the numerical value θ_ξ with (5).

Step 3: Construct the Binary Adjacency Matrix

This step aims to determine the binary adjacency matrix Θ, which represents the relationships among agents.

Step 4: Calculate the Difference Between Information

The difference between the information of agent i and agent j at time t is:

$$D(\upsilon_i(t), \upsilon_j(t)) = |\upsilon_i(t) - \upsilon_j(t)| \tag{7}$$

Step 5: Calculate the Hyperbolic Tangent Function

The hyperbolic tangent function is smooth and continuous, and it maps input values to a range between -1 and 1, which makes it helpful in controlling the influence of large or small inputs. The expression is:

$$f(x) = \frac{e^x - e^{-x}}{e^x + e^{-x}} \tag{8}$$

To map the range to the interval $[0,1]$, the function is improved to the following form:

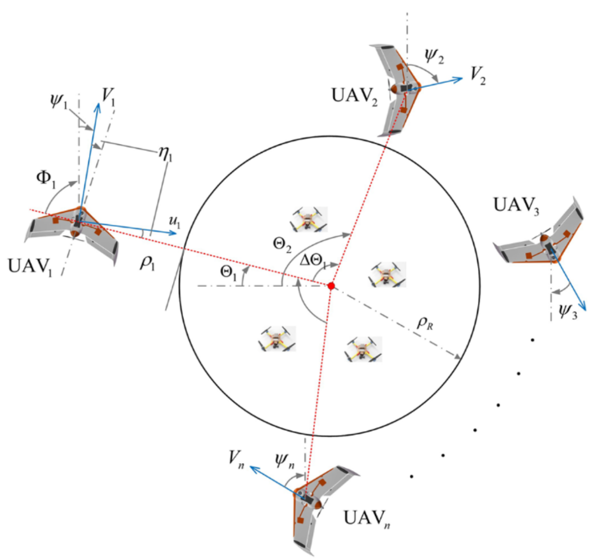

Fig. 1: Circumnavigation of m Targets by n UAVs (Red Center Represents the Geometric Centroid of m Targets) [39].

$$\begin{aligned} g(x) &= \frac{1}{2}\left(f(x-\eta)+1\right) \\ &= \frac{1}{2}\left(\frac{e^{(x-\eta)} - e^{-(x-\eta)}}{e^{(x-\eta)} + e^{-(x-\eta)}} + 1\right),\ \eta \geq 0 \end{aligned} \tag{9}$$

where x is the reciprocal of $D(\upsilon_i(t), \upsilon_j(t))$. Especially, $g(x) = 1$ when $\upsilon_i(t) = \upsilon_j(t)$.

Step 6: Determine the Weights of Agents

The weight ω_{ij} of agent e_j in agent e_i's information update process is:

$$\omega_{ij}(t) = \frac{g\left(\frac{1}{D(\upsilon_i(t), \upsilon_j(t))}\right)}{\sum_{k=1}^{N} g\left(\frac{1}{D(\upsilon_k(t), \upsilon_i(t))}\right)} \tag{10}$$

Step 7: Information Evolution.

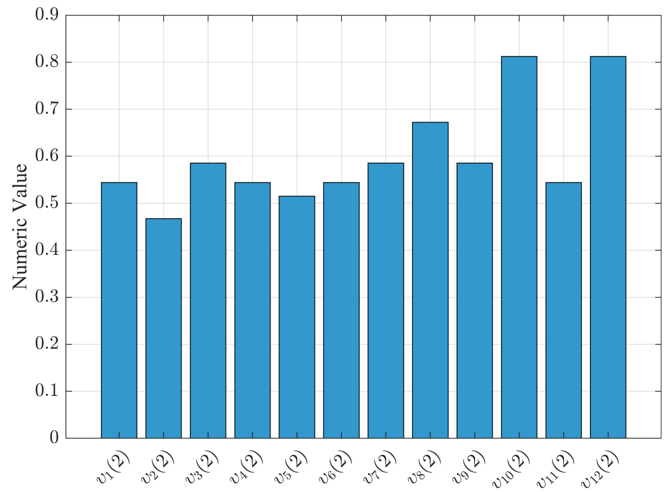

Fig. 2: Numeric Values of Each Agent at $t = 2$.

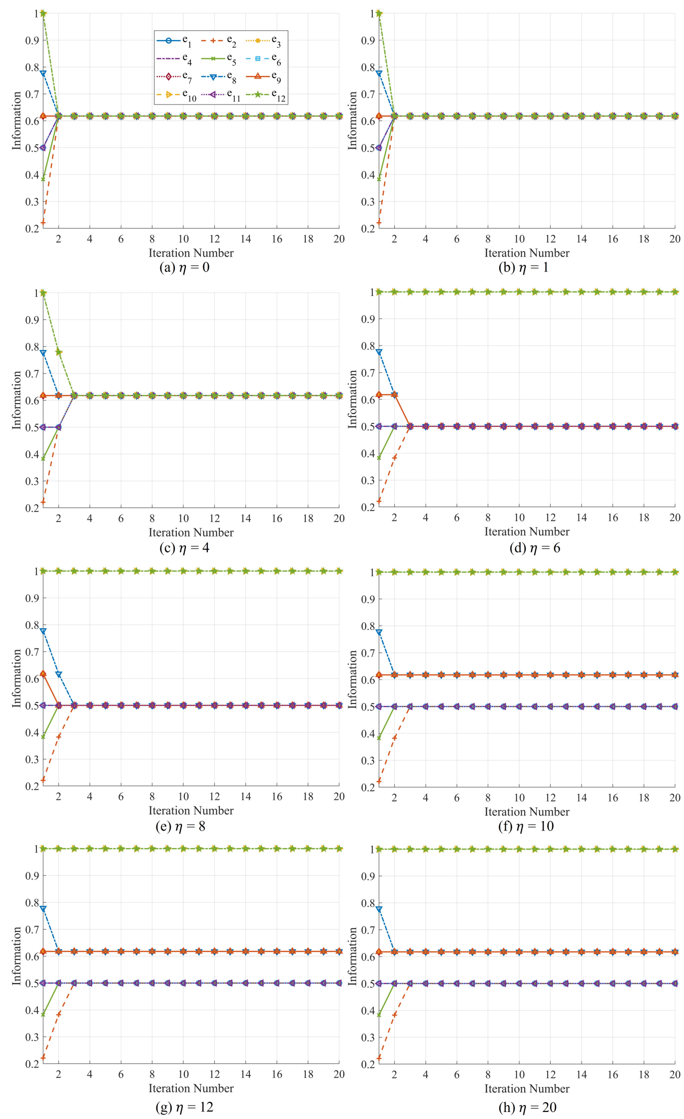

Fig. 3: Information Update of Each Agent As η Varies.

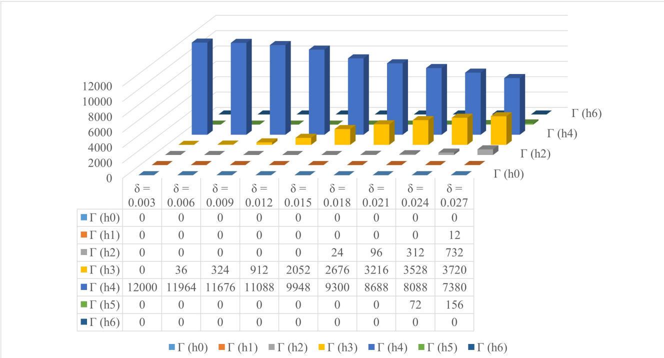

	δ = 0.003	δ = 0.006	δ = 0.009	δ = 0.012	δ = 0.015	δ = 0.018	δ = 0.021	δ = 0.024	δ = 0.027
Γ (h0)	0	0	0	0	0	0	0	0	0
Γ (h1)	0	0	0	0	0	0	0	0	12
Γ (h2)	0	0	0	0	0	24	96	312	732
Γ (h3)	0	36	324	912	2052	2676	3216	3528	3720
Γ (h4)	12000	11964	11676	11088	9948	9300	8688	8088	7380
Γ (h5)	0	0	0	0	0	0	0	72	156
Γ (h6)	0	0	0	0	0	0	0	0	0

Fig. 4: Statistical Results Under Different Noise Intensities.

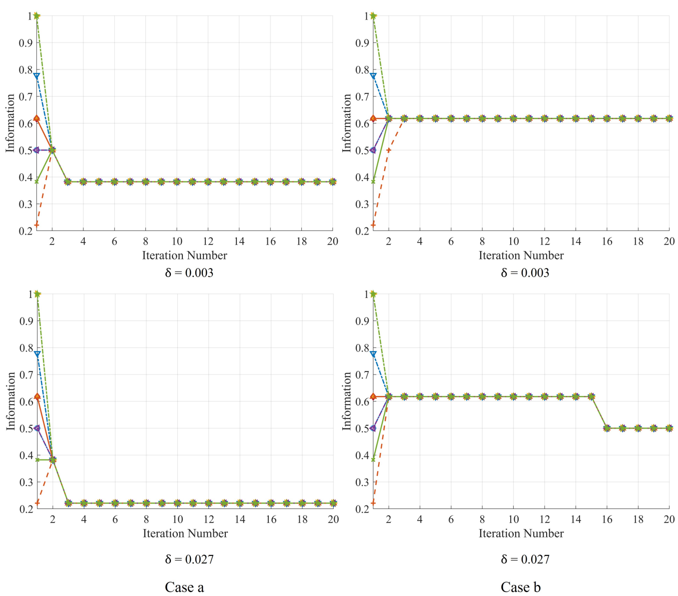

Fig. 5: Agent Information Update Processes Under Different Noise Intensities and Weight Selection Methods.

$\upsilon_i(t+1)$ is the numerical value of e_i's information at time $t+1$, then:

$$\upsilon_i(t+1) = \sum_{k=1}^{N} \omega_{ik}(t)\upsilon_k(t) + \mathcal{N}(\mu, \delta^2) \tag{11}$$

The linguistic expression is defined:

$$\Upsilon_i(t+1) = \upsilon^{-1}(\upsilon_i(t+1)) \tag{12}$$

where

$$\begin{aligned} &\upsilon^{-1}(\upsilon_i(t+1)) \\ &= \begin{cases} h_{2\Phi}, & \upsilon_i(t+1) \geq 1; \\ \underset{\theta_\xi \in H}{\arg\min} |\upsilon_i(t+1) - \theta_\xi|, & 0 < \upsilon_i(t+1) < 1; \\ h_0, & \upsilon_i(t+1) \leq 0. \end{cases} \end{aligned} \tag{13}$$

Step 8: Iterative Simulation and Result Recording

Repeat the process from *Step 4* to *Step 7*. In each iteration, we simulate the interactions of N agents to model the information evolution, continuing until the number of iterations T is reached. At the end of this round, we record the final information of the agent e_n as $\kappa_n(T)$. To ensure the robustness of the results, repeat the test M times, each time independently simulating the evolution of agents' information. We then record the linguistic term h_ξ that occurs in the entire test and then count the number of times, denoted as $\Gamma(h_\xi)$.

Algorithm 1 Information Evolution Based on Social Network, Hyperbolic Tangent Function, and Monte Carlo Method

Input: Number of agents N, iteration limit T, number of simulations M, LTS $H = \{h_\xi\}$, initial information.
Output: $\kappa_n(T)$, frequency count $\Gamma(h_\xi)$.
for $m = 1$ to M **do**
  Initialize $\Upsilon_n(1)$ and compute $\upsilon_n(1)$ for all agents
  Determine the binary adjacency matrix Θ
  for $t = 1$ to T **do**
    for each agent e_i **do**
      for each agent e_j **do**
        Compute $D(\upsilon_i(t), \upsilon_j(t)) = |\upsilon_i(t) - \upsilon_j(t)|$
        Compute $x = \frac{1}{D(\upsilon_i(t), \upsilon_j(t))}$
        Compute $g(x) = \frac{1}{2}\left(\frac{e^{(x-\eta)} - e^{-(x-\eta)}}{e^{(x-\eta)} + e^{-(x-\eta)}} + 1\right)$
      end for
      Compute weights: $\omega_{ij}(t) = \frac{g(\frac{1}{D(\upsilon_i(t), \upsilon_j(t))})}{\sum_{k=1}^{N} g(\frac{1}{D(\upsilon_k(t), \upsilon_i(t))})}$
    end for
    for each agent e_i **do**
      Update numeric value: $\upsilon_i(t+1) = \sum_{k=1}^{N} \omega_{ik}(t)\upsilon_k(t) + \mathcal{N}(\mu, \delta^2)$
      Map back to linguistic term:
$$\Upsilon_i(t+1) = \begin{cases} h_{2\Phi}, & \upsilon_i(t+1) \geq 1 \\ \arg\min_{\theta_\xi \in H} |\upsilon_i(t+1) - \theta_\xi|, & 0 < \upsilon_i(t+1) < 1 \\ h_0, & \upsilon_i(t+1) \leq 0 \end{cases}$$
    end for
  end for
  Record $\kappa_n(T) = \upsilon_n(T)$ for each agent e_n
  Update frequency count $\Gamma(h_\xi)$ for all observed h_ξ
end for

To further analyze and validate the proposed algorithm, we present several theorems in the Appendix. For simplicity and clarity, noise is not considered in the theoretical analysis.

IV. Numerical Example

A. *Example for Multi-UAV Cooperative Decision-Making*

Assume that $N = 12$ agents $e_1, e_2, \cdots, e_{12}$ are deployed to a disaster site. These UAVs fly to the area and position themselves around the scene, forming a surrounding monitoring pattern. This setup allows for real-time observation from different angles. However, because each drone has a different position in the air and may carry sensors with varying levels of accuracy, the information they collect about the scene may vary. The LTS is $H = \{h_0 = \text{very poor}, h_1 = \text{poor}, h_2 = \text{slightly poor}, h_3 = \text{fair}, h_4 = \text{slightly good}, h_5 = \text{good}, h_6 = \text{very good}\}$. We set $T = 20$ and $M = 1000$. The noise is $X \sim \mathcal{N}(0, 0.003^2)$. In this example, it is assumed that any two agents in the multi-agent system can communicate and exchange information effectively.

Step 1: Initialization

The initial evaluation information is $\Upsilon_1(1) = h_3$, $\Upsilon_2(1) = h_1$, $\Upsilon_3(1) = h_4$, $\Upsilon_4(1) = h_3$, $\Upsilon_5(1) = h_2$, $\Upsilon_6(1) = h_3$, $\Upsilon_7(1) = h_4$, $\Upsilon_8(1) = h_5$, $\Upsilon_9(1) = h_4$, $\Upsilon_{10}(1) = h_6$, $\Upsilon_{11}(1) = h_3$, $\Upsilon_{12}(1) = h_6$.

Step 2: Transform Linguistic Terms into Numerical Values

The value of a in (5) is 1.37. The numerical values of linguistic terms are $\theta_0 = 0$, $\theta_1 = 0.2210$, $\theta_2 = 0.3823$, $\theta_3 = 0.50$, $\theta_4 = 0.6177$, $\theta_5 = 0.7790$, and $\theta_6 = 1$. Therefore, $\upsilon_1(1) = 0.50$, $\upsilon_2(1) = 0.2210$, $\upsilon_3(1) = 0.6177$, $\upsilon_4(1) = 0.50$, $\upsilon_5(1) = 0.3823$, $\upsilon_6(1) = 0.50$, $\upsilon_7(1) = 0.6177$, $\upsilon_8(1) = 0.7790$, $\upsilon_9(1) = 0.6177$, $\upsilon_{10}(1) = 1$, $\upsilon_{11}(1) = 0.50$, $\upsilon_{12}(1) = 1$.

Step 3: Construct the Binary Adjacency Matrix

Since all agents in this example can exchange information normally, the binary adjacency matrix is $\Theta = \mathbf{1}_{12\times 12}$.

Step 4: Calculate the Difference Between Information

The difference between the information of agent i and agent j at time $t = 1$ is shown in Table I.

TABLE I: Distance Between Linguistic Information at $t = 1$.

$D(\upsilon_i(1), \upsilon_j(1))$	e_1	e_2	e_3	e_4	e_5	e_6	e_7	e_8	e_9	e_{10}	e_{11}	e_{12}
e_1	0	0.2790	0.1177	0	0.1177	0	0.1177	0.2790	0.1177	0.50	0	0.50
e_2	0.2790	0	0.3967	0.2790	0.1613	0.2790	0.3967	0.5580	0.3967	0.7790	0.2790	0.7790
e_3	0.1177	0.3967	0	0.1177	0.2354	0.1177	0	0.1613	0	0.3823	0.1177	0.3823
e_4	0	0.2790	0.1177	0	0.1177	0	0.1177	0.2790	0.1177	0.50	0	0.50
e_5	0.1177	0.1613	0.2354	0.1177	0	0.1177	0.2354	0.3967	0.2354	0.6177	0.1177	0.6177
e_6	0	0.2790	0.1177	0	0.1177	0	0.1177	0.2790	0.1177	0.50	0	0.50
e_7	0.1177	0.3967	0	0.1177	0.2354	0.1177	0	0.1613	0	0.3823	0.1177	0.3823
e_8	0.2790	0.5580	0.1613	0.2790	0.3967	0.2790	0.1613	0	0.1613	0.2210	0.2790	0.2210
e_9	0.1177	0.3967	0	0.1177	0.2354	0.1177	0	0.1613	0	0.3823	0.1177	0.3823
e_{10}	0.50	0.7790	0.3823	0.50	0.6177	0.50	0.3823	0.2210	0.3823	0	0.50	0
e_{11}	0	0.2790	0.1177	0	0.1177	0	0.1177	0.2790	0.1177	0.50	0	0.50
e_{12}	0.50	0.7790	0.3823	0.50	0.6177	0.50	0.3823	0.2210	0.3823	0	0.50	0

Step 5: Calculate the Hyperbolic Tangent Function

The value of hyperbolic tangent function at $t = 1$ is shown in Table II.

TABLE II: Value of Hyperbolic Tangent Function.

$g(\frac{1}{D(\upsilon_i(1),\upsilon_j(1))})$	e_1	e_2	e_3	e_4	e_5	e_6	e_7	e_8	e_9	e_{10}	e_{11}	e_{12}
e_1	1	0.7629	1	1	1	1	1	0.7629	1.0000	0.1192	1.0000	0.1192
e_2	0.7629	1	0.2772	0.7629	0.9983	0.7629	0.2772	0.0820	0.2772	0.0313	0.7629	0.0313
e_3	1	0.2772	1	1	0.9239	1	1	0.9983	1	0.3168	1	0.3168
e_4	1	0.7629	1	1	1	1	1	0.7629	1	0.1192	1	0.1192
e_5	1	0.9983	0.9239	1	1	1	0.9239	0.2772	0.9239	0.0594	1	0.0594
e_6	1	0.7629	1	1	1	1	1	0.7629	1	0.1192	1	0.1192
e_7	1	0.2772	1	1	0.9239	1	1	0.9983	1	0.3168	1	0.3168
e_8	0.7629	0.0820	0.9983	0.7629	0.2772	0.7629	0.9983	1	0.9983	0.9548	0.7629	0.9548
e_9	1	0.2772	1	1	0.9239	1	1	0.9983	1	0.3168	1	0.3168
e_{10}	0.1192	0.0313	0.3168	0.1192	0.0594	0.1192	0.3168	0.9548	0.3168	1	0.1192	1
e_{11}	1	0.7629	1	1	1	1	1	0.7629	1	0.1192	1	0.1192
e_{12}	0.1192	0.0313	0.3168	0.1192	0.0594	0.1192	0.3168	0.9548	0.3168	1	0.1192	1

Step 6: Determine the Weights of Agents

The weight ω_{ij} of agent e_j in agent e_i's information update process is shown in Table III.

Step 7: Information Evolution.

According to (11), we can obtain the numeric values of each agent at $t = 2$, as shown in Fig. 2. Based on (12) and (13), we can obtain $\Upsilon_1(2) = h_3$, $\Upsilon_2(2) = h_3$, $\Upsilon_3(2) = h_4$, $\Upsilon_4(2) = h_3$, $\Upsilon_5(2) = h_3$, $\Upsilon_6(2) = h_3$, $\Upsilon_7(2) = h_4$, $\Upsilon_8(2) = h_4$, $\Upsilon_9(2) = h_4$, $\Upsilon_{10}(2) = h_5$, $\Upsilon_{11}(2) = h_3$, and $\Upsilon_{12}(2) = h_5$.

Step 8: Iterative Simulation and Result Recording

After tests, we can obtain $\Gamma(h_0) = \Gamma(h_1) = \Gamma(h_2) = \Gamma(h_3) = \Gamma(h_5) = \Gamma(h_6) = 0$ and $\Gamma(h_4) = NM = 12000$. The final information is h_4.

TABLE III: Weights of Each Agent in the First Iteration.

ω_{ij}	e_1	e_2	e_3	e_4	e_5	e_6	e_7	e_8	e_9	e_{10}	e_{11}	e_{12}
e_1	0.1024	0.1266	0.1017	0.1024	0.1091	0.1024	0.1017	0.0819	0.1017	0.0267	0.1024	0.0267
e_2	0.0781	0.1659	0.0282	0.0781	0.1089	0.0781	0.0282	0.0088	0.0282	0.0070	0.0781	0.0070
e_3	0.1024	0.0460	0.1017	0.1024	0.1008	0.1024	0.1017	0.1072	0.1017	0.0708	0.1024	0.0708
e_4	0.1024	0.1266	0.1017	0.1024	0.1091	0.1024	0.1017	0.0819	0.1017	0.0267	0.1024	0.0267
e_5	0.1024	0.1657	0.0940	0.1024	0.1091	0.1024	0.0940	0.0298	0.0940	0.0133	0.1024	0.0133
e_6	0.1024	0.1266	0.1017	0.1024	0.1091	0.1024	0.1017	0.0819	0.1017	0.0267	0.1024	0.0267
e_7	0.1024	0.0460	0.1017	0.1024	0.1008	0.1024	0.1017	0.1072	0.1017	0.0708	0.1024	0.0708
e_8	0.0781	0.0136	0.1015	0.0781	0.0302	0.0781	0.1015	0.1074	0.1015	0.2135	0.0781	0.2135
e_9	0.1024	0.0460	0.1017	0.1024	0.1008	0.1024	0.1017	0.1072	0.1017	0.0708	0.1024	0.0708
e_{10}	0.0122	0.0052	0.0322	0.0122	0.0065	0.0122	0.0322	0.1025	0.0322	0.2236	0.0122	0.2236
e_{11}	0.1024	0.1266	0.1017	0.1024	0.1091	0.1024	0.1017	0.0819	0.1017	0.0267	0.1024	0.0267
e_{12}	0.0122	0.0052	0.0322	0.0122	0.0065	0.0122	0.0322	0.1025	0.0322	0.2236	0.0122	0.2236

B. *Example for Theorem 1*

The initial information used in this example is the same with *Example for Multi-UAV Cooperative Decision-Making*.

1) By setting $\eta = 2$, we can calculate that the weight assigned to e_4, who shares the same information as e_1, is $\omega_{14}(2) = \frac{g\left(\frac{1}{D(\upsilon_1(1),\upsilon_4(1))}\right)}{\sum_{k=2}^{15} g\left(\frac{1}{D(\upsilon_k(1),\upsilon_1(1))}\right)} = \frac{1}{9.9193} = 0.1008$. Similarly, when $\eta = 4$, $\omega_{14}(2) = \frac{g\left(\frac{1}{D(\upsilon_1(1),\upsilon_4(1))}\right)}{\sum_{k=2}^{15} g\left(\frac{1}{D(\upsilon_k(1),\upsilon_1(1))}\right)} = \frac{1}{7.6421} = 0.1309$. It can be seen that as η increases, ω_{14} increases, which confirms *Theorem 1*.

2) To verify the important role played by η, we verify a total of eight cases when η takes the value of 0, 1, 4, 6, 8, 10, 12, and 20. The results are shown in Fig. 3. It can be seen that in the first three cases, all agents finally reach a consensus. However, as η gradually increases, the information diverges. An important reason for this situation is that when η is small, the confidence threshold of the agents is substantial. Even information with significant differences will be updated, which is similar to the DeGroot model mentioned above. A distinctive characteristic of the DeGroot model is its tendency for agents to reach a consensus, irrespective of their initial information, ultimately. As η increases, the influence of information with significant differences diminishes gradually, akin to establishing a confidence threshold ε in the bounded confidence model. This transition gradually aligns the model with the behavior of the HK model.

C. *Example for Theorem 2*

The parameter settings in this example are consistent with those in *Example for Theorem 1*. Specifically, $\eta = 2$. From the results presented in Table IV, it is evident that initially, in the first iteration, the information of the agents varies. However, starting from the second iteration, all agents' information rapidly converges to a standard value, 0.4422, and remains constant in subsequent iterations, including the twentieth and beyond. This observation indicates the existence of a stable state of opinion agreement in the model. Once the agents' information becomes identical at a certain point in time, they remain the same indefinitely. Therefore, the simulation results validate *Theorem 2*, demonstrating the model's characteristics of information consensus and stability.

TABLE IV: Information of Each Agent in *Example for Theorem 2*.

Iteration	e_1	e_2	e_3	e_4	e_5	e_6	e_7	e_8	e_9	e_{10}	e_{11}	e_{12}
1	0.5	0.5	0.5	0.5	0.5	0.5	0.5	0.5	0.5	0.5	0.5	1
2	0.5	0.5	0.5	0.5	0.5	0.5	0.5	0.5	0.5	0.5	0.5	0.5
3	0.5	0.5	0.5	0.5	0.5	0.5	0.5	0.5	0.5	0.5	0.5	0.5
⋮	⋮	⋮	⋮	⋮	⋮	⋮	⋮	⋮	⋮	⋮		
20	0.5	0.5	0.5	0.5	0.5	0.5	0.5	0.5	0.5	0.5	0.5	0.5

D. *Example for Theorem 3*

Suppose that eleven agents have the same initial information $\Upsilon_1(1) = \Upsilon_2(1) = \cdots = \Upsilon_{11}(1) = h_3$, and the agent e_{12} has the initial information $\Upsilon_{12}(1) = h_6$. The information evolution can be seen in Table V. It can be seen that the information of all agents reaches the consensus h_3 in the second iteration, which confirms *Theorem 3*.

TABLE V: Opinion Values of Each Agent in Each Iteration When $\chi = 11$ and $\psi = 1$.

Iteration	e_1	e_2	e_3	e_4	e_5	e_6	e_7	e_8	e_9	e_{10}	e_{11}	e_{12}
1	0.5	0.5	0.5	0.5	0.5	0.5	0.5	0.5	0.5	0.5	0.5	1
2	0.5	0.5	0.5	0.5	0.5	0.5	0.5	0.5	0.5	0.5	0.5	0.5
3	0.5	0.5	0.5	0.5	0.5	0.5	0.5	0.5	0.5	0.5	0.5	0.5
⋮	⋮	⋮	⋮	⋮	⋮	⋮	⋮	⋮	⋮	⋮		
20	0.5	0.5	0.5	0.5	0.5	0.5	0.5	0.5	0.5	0.5	0.5	0.5

E. *Example for Theorem 4*

Based on *Example for Theorem 3*, the number of χ is changed from eleven to six, i.e., $\Upsilon_i(1) = h_3,\ i = 1, 2, \cdots, 6$ and $\Upsilon_j(1) = h_6,\ j = 7, 8, \cdots, 12$. The rest remain the same. The results are shown in Table VI. Besides, we set $\chi = 5$ and $\psi = 7$. The rest remain the same. The results are shown in Table VII. It can be observed that the agents fail to reach a consensus when $\chi = 6$ and $\psi = 6$, whereas they do reach a consensus when $\chi = 5$ and $\psi = 7$. This indicates that the ability of the agents to reach a consensus is influenced by the values of χ and ψ, thus confirming *Theorem 4*.

TABLE VI: Information of Each Agent in Each Iteration When $\chi = 6$ and $\psi = 6$.

Iteration	e_1	e_2	e_3	e_4	e_5	e_6	e_7	e_8	e_9	e_{10}	e_{11}	e_{12}
1	0.5	0.5	0.5	0.5	0.5	0.5	1	1	1	1	1	1
2	0.6177	0.6177	0.6177	0.6177	0.6177	0.6177	0.7790	0.7790	0.7790	0.7790	0.7790	0.7790
3	0.7790	0.7790	0.7790	0.7790	0.7790	0.7790	0.6177	0.6177	0.6177	0.6177	0.6177	0.6177
4	0.6177	0.6177	0.6177	0.6177	0.6177	0.6177	0.7790	0.7790	0.7790	0.7790	0.7790	0.7790
5	0.7790	0.7790	0.7790	0.7790	0.7790	0.7790	0.6177	0.6177	0.6177	0.6177	0.6177	0.6177
6	0.6177	0.6177	0.6177	0.6177	0.6177	0.6177	0.7790	0.7790	0.7790	0.7790	0.7790	0.7790
⋮	⋮	⋮	⋮	⋮	⋮	⋮	⋮	⋮	⋮	⋮		
19	0.7790	0.7790	0.7790	0.7790	0.7790	0.7790	0.6177	0.6177	0.6177	0.6177	0.6177	0.6177
20	0.6177	0.6177	0.6177	0.6177	0.6177	0.6177	0.7790	0.7790	0.7790	0.7790	0.7790	0.7790

F. *Example for Theorem 5*

Here, we adopt the case with $\chi = 5$ and $\psi = 7$ in *Example for Theorem 4* to illustrate the behavior of the system. Therefore, $\chi = 5$, $\psi = 7$, $h_{\xi_1} = h_3$, and $h_{\xi_2} = h_6$.

TABLE VII: Information of Each Agent in Each Iteration When $\chi = 5$ and $\psi = 7$.

Iteration	e_1	e_2	e_3	e_4	e_5	e_6	e_7	e_8	e_9	e_{10}	e_{11}	e_{12}
1	0.5	0.5	0.5	0.5	0.5	1	1	1	1	1	1	1
2	0.7790	0.7790	0.7790	0.7790	0.7790	0.7790	0.7790	0.7790	0.7790	0.7790	0.7790	0.7790
3	0.7790	0.7790	0.7790	0.7790	0.7790	0.7790	0.7790	0.7790	0.7790	0.7790	0.7790	0.7790
⋮	⋮	⋮	⋮	⋮	⋮	⋮	⋮	⋮	⋮	⋮		
20	0.7790	0.7790	0.7790	0.7790	0.7790	0.7790	0.7790	0.7790	0.7790	0.7790	0.7790	0.7790

Then, $\alpha = (\chi - 1) + g\left(\frac{1}{D(h_{\xi_1}, h_{\xi_2})}\right)\psi = 4 + 0.5 * 7 = 7.5$ and $\beta = (\psi - 1) + g\left(\frac{1}{D(h_{\xi_1}, h_{\xi_2})}\right)\chi = 6 + 0.5 * 5 = 8.5$. It is can be obtained that $\upsilon_i(2) = \frac{\chi-1}{\alpha}\upsilon_i(1) + \left(1 - \frac{\chi-1}{\alpha}\right)\upsilon_j(1) = \frac{4}{7.5} * 0.5 + (1 - \frac{4}{7.5}) * 1 = 0.7333$ and $\upsilon_j(2) = \left(1 - \frac{\psi-1}{\beta}\right)\upsilon_i(1) + \frac{\psi-1}{\beta}\upsilon_j(1) = (1 - \frac{6}{8.5}) * 0.5 + \frac{6}{8.5} * 1 = 0.8529$. The value $|\upsilon_j(t+1) - \upsilon_i(t+1)| = 0.1196$ is relatively small, indicating that the system reaches consensus by the second iteration, as shown in Table VII. The above results confirm *Theorem 5*.

V. Comparison Analysis and Potential Applications

In this section, we will compare the proposed model with several models and conduct the robustness test.

A. *Comparison Analysis*

1) System Performance Under Different Noise Intensities: To assess the system's performance under different levels of noise interference and evaluate its robustness, we conducted nine sets of experiments, introducing noise with standard deviations of 0.003, 0.006, 0.009, 0.012, 0.015, 0.018, 0.021, 0.024, and 0.027, respectively. It is important to note that since the LSFs used in this study have a value range of [0,1], a standard deviation of 0.027 represents a relatively strong disturbance. The information update process of each agent under different noise levels can be seen in Supplyment Materia. Fig. 4 shows that when the noise intensity is low, all agents eventually converge to the same opinion, h_4. This indicates that the proposed model can maintain stable results even in a noisy environment and is not significantly affected by minor disturbances. As the noise intensity increases, the agents' information states begin to shift, no longer fully converging to h_4 but instead showing a distribution around h_3 and h_5. This suggests that higher noise levels impact the convergence process to some extent. However, even under strong noise interference, the system's final results still fluctuate only slightly around h_4 without significant deviation. This demonstrates that the proposed model maintains strong robustness against high-intensity noise and ensures a stable decision-making trend even in extreme conditions.

2) Impact of Different LSFs on Information Updating: In different research fields, such as decision analysis and sentiment analysis, the choice of LSFs directly influences how information is expressed and how data is processed. Different applications require varying levels of accuracy and detail in linguistic scales. For example, in market research, finer scales help capture small differences in consumer attitudes, while in risk assessment or expert decision-making, broader scales are often preferred to enhance clarity and consistency in judgments. Therefore, using different LSFs not only meets the specific needs of various fields but also improves the model's versatility and adaptability across different applications.

In this study, we also adopt three other types of LSFs $\theta_1 = \frac{\xi}{2\Phi}$, $\theta_2 = \left(\frac{\xi}{2\Phi}\right)^{\Phi}$, and $\theta_3 = \left(\frac{\xi}{2\Phi}\right)^{\frac{1}{\Phi}}$, $(\xi = 0, 1, \cdots, 2\Phi)$ for comparison and applied noise interference of varying intensities. Due to space limitations, the figure illustrating the information update process of each agent under different LSFs is presented at Supplyment Materia. The results show that even when the agent's evaluation information remains the same, different LSFs still lead to significant differences in the final results. This confirms an important point: although the evaluation data itself does not change, the meaning it conveys varies across different LSFs. This finding further demonstrates that the proposed model can be flexibly applied to different fields based on specific needs. Additionally, the results show that under the same LSFs, increasing the noise intensity does not cause major changes in the final results. This further proves that the proposed model maintains a stable decision-making trend, even under substantial noise interference, highlighting its robustness and resistance to disturbances.

3) Comparison with Traditional DeGroot Model: In the DeGroot model, the agents unconditionally trust the other agents [23]. Suppose that $E = \{e_1, e_2, \cdots, e_N\}$ indicates the agents. $t \in \{1, 2, \cdots, T\}$ indicates the discrete variable representing the number of rounds of opinion evolution. $\upsilon_k(t) \in [0, 1]$ is the numeric opinion at time t. The weight of e_j in e_i's information update process is ω_{ij}. The numerical value of e_i's information at time $t+1$ is $\upsilon_i(t+1) = \sum_{k=1}^{N} \omega_{ik}(t)\upsilon_k(t)$.In this part, we set two scenarios for the weight vector of agents. In Case (a), the weight vector of agents is $\Omega = \{\omega_1, \omega_2, \cdots, \omega_{15}\} = \{\frac{1}{15}, \frac{1}{15}, \cdots, \frac{1}{15}\}$. In Case (b), the agents' weight vector when e_i updates the information is based on the distance between opinions $\omega_j = \frac{e^{-|D_{ij}|}}{\sum_{k=1}^{15} e^{-|D_{ik}|}}$. Other settings are consistent with the example in the Numerical Example section.

In this study, different levels of noise are applied to Case a and Case b, specifically 0.003 and 0.027, respectively. The results are shown in Supplyment Materia. It can be seen that when the noise intensity is 0.003, the final results under the two different weight selection methods exhibit significant discrepancies. Furthermore, when the weight calculation method for the agents remains unchanged, increasing the system's noise intensity leads to substantial variations in the results. These findings indicate that the DeGroot model lacks robustness and exhibits poor resistance to external disturbances. However, as shown in Fig. 4, with the increase in noise intensity, the results obtained based on the proposed model do not exhibit significant fluctuations, which demonstrates that the model possesses a certain degree of robustness against disturbances.

4) Comparison with Traditional HK Model: The description of the HK model can be seen in *Definition 2*. The test consists of 16 subplots, representing the results under four different values of the confidence bound parameter ε: 0, 0.25, 0.5, and 0.9. The results are shown in the Supplemental Materials. For each ε value, four different noise levels are tested: 0, 0.003, 0.015, and 0.027. When $\varepsilon = 0$, each agent completely rejects exchanging opinions with its neighbors. As the noise intensity increases, however, noticeable changes emerge. Specifically, when the noise level reaches 0.027, some agents begin to converge in their opinions. This indicates that a certain level of noise can break the "information cocoon" effect, allowing communication and agreement to emerge among agents who would otherwise remain isolated. As the value of ε increases, we observe that the final opinions become more consistent across agents. These results demonstrate that the HK model is susceptible to the choice of ε. Even slight changes in ε can lead to significantly different outcomes. This sensitivity poses a significant limitation for practical applications, as ε is often determined subjectively by decision-makers. Identifying the most appropriate value for ε remains a difficult task, especially in large-scale decision-making scenarios where more complex factors must be taken into account.

B. *Potential Applications of Proposed Model*

The proposed model demonstrates strong potential for application in various real-world scenarios. Below, several representative use cases are presented to illustrate the practical value and adaptability.

In urban stability maintenance, multiple UAVs can be deployed collaboratively at the scene of emergencies such as riots, fires, or explosions. Due to differences in sensor accuracy, flight perspectives, and environmental conditions, each UAV may generate a different initial assessment of the event's severity. By applying the model proposed in this paper, it is possible to simulate the exchange and evolution of information among UAVs, integrate multi-source data, and ultimately reach a consistent evaluation of the event. This provides a more reliable foundation for decision-making in command and control centers.

In wildlife conservation and ecological monitoring, UAVs can be used for long-range tracking and behavior analysis of animal populations. When dealing with complex terrain, partial visual obstruction, or unclear behavior patterns, different UAVs may form inconsistent judgments about whether animals are migrating, foraging, gathering, or reacting to external disturbances. The proposed model enables the dynamic exchange and refinement of this information, improving the overall accuracy in identifying group behavior and offering intelligent support for ecological research and wildlife management.

In military operations, particularly in air combat scenarios involving multiple autonomous agents, UAVs independently assess the current situation based on local observations, including the force distribution, positional advantage, and firepower balance. However, due to incomplete or noisy information, these assessments may conflict with one another. By applying the proposed model, it is possible to simulate the cognitive interaction process among UAVs, reach consensus on the combat situation, and enhance the effectiveness of battlefield decisions.

VI. Conclusion

This paper proposes a novel information fusion model for multi-UAV cooperative decision-making. The model integrates a social network structure to simulate the communication among agents, a hyperbolic tangent function to adjust weights based on linguistic information distance dynamically, and the Monte Carlo method to evaluate performance under a noisy and uncertain environment. Unlike traditional models such as the DeGroot and HK models, the proposed model offers improved adaptability in complex environments and better support for processing different types of linguistic information. The model also introduces a dynamic weighting mechanism that reflects the degree of agreement among agents. Through simulation studies, the model demonstrates the advantages in terms of resistance to noise and stability of results. These contributions highlight the model's potential as a practical and effective tool for enhancing the decision-making ability in multi-agent systems.

The model proposed in this paper may exhibit deviations in the final results under strong noise interference. As a next step, we plan to explore the use of artificial intelligence techniques for information compensation and correction, such as recurrent neural networks or reinforcement learning. Besides, since the paper is related to evaluation under uncertainty, further research will also explore advanced uncertainty modeling techniques, such as type-2 fuzzy sets or probabilistic linguistic terms, to enhance the model's ability to handle uncertain information in real-world scenarios. We will also consider scenarios where communication is limited to partial or local interactions among agents, rather than assuming global communication availability.

Acknowledgment

Appendix

Theorem 1:

1) As η increases, the weights of agents with the same information increase;

2) A large η indicates that an agent mainly considers the information of those who exhibit a significant degree of consensus with its own information. In the HK model, this corresponds to setting a very small threshold value ε. Conversely, a small η indicates that ε is set to a large value, allowing the agent to accept information from others that may significantly diverge from its own.

Proof:

1) Suppose that the agents e_i and e_j have the same information at time t, i.e., $D(\Upsilon_i(t),\Upsilon_j(t))=0$, then

$$g_1\Big(\frac{1}{D(\Upsilon_i(t),\Upsilon_j(t))}\Big)=g_2\Big(\frac{1}{D(\Upsilon_i(t),\Upsilon_j(t))}\Big)=1$$

If $\eta_1>\eta_2$, then

$$\sum_{k=1,k\neq i}^{N} g_1\Big(\frac{1}{D(\Upsilon_i(t),\Upsilon_k(t))}\Big)<\sum_{k=1,k\neq i}^{N} g_2\Big(\frac{1}{D(\Upsilon_i(t),\Upsilon_k(t))}\Big)$$

Therefore,

$$\frac{g_1\Big(\frac{1}{D(\Upsilon_i(t),\Upsilon_j(t))}\Big)}{\sum_{k=1,k\neq i}^{N} g_1\Big(\frac{1}{D(\Upsilon_i(t),\Upsilon_k(t))}\Big)}>\frac{g_2\Big(\frac{1}{D(\Upsilon_i(t),\Upsilon_j(t))}\Big)}{\sum_{k=1,k\neq i}^{N} g_2\Big(\frac{1}{D(\Upsilon_i(t),\Upsilon_k(t))}\Big)}$$

2) Suopose now $D(\Upsilon_i(t),\Upsilon_j(t))\neq 0$;

Let $b_j=e^{-\frac{2}{D(\Upsilon_i(t),\Upsilon_j(t))}}$ and $b_k=e^{-\frac{2}{D(\Upsilon_i(t),\Upsilon_k(t))}}$, $k=1,2,\cdots,N; k\neq i; b_j,b_k\in(0,\frac{1}{e^2}]$.

$$\omega_{ij}=\frac{g\Big(\frac{1}{D(\Upsilon_i(t),\Upsilon_j(t))}\Big)}{\sum_{k=1,k\neq i}^{N} g\Big(\frac{1}{D(\Upsilon_i(t),\Upsilon_k(t))}\Big)}=\frac{\frac{1}{1+e^{-2\left(\frac{1}{D(\Upsilon_i(t),\Upsilon_j(t))}\right)+2\eta}}}{\sum_{k=1,k\neq i}^{N}\frac{1}{1+e^{-2\left(\frac{1}{D(\Upsilon_i(t),\Upsilon_k(t))}\right)+2\eta}}}$$

$$=\frac{\frac{1}{1+b_je^{2\eta}}}{\sum_{k=1,k\neq i}^{N}\frac{1}{1+b_ke^{2\eta}}}=\frac{1}{\sum_{k=1,k\neq i}^{N}\frac{1+b_je^{2\eta}}{1+b_ke^{2\eta}}}$$

Here, we consider two special cases.

- $\Upsilon_j(t)$ and $\Upsilon_i(t)$ are pretty different and the other information $\Upsilon_k(t)$ are all pretty close to $\Upsilon_i(t)$, i.e., $\lim D(\Upsilon_i(t),\Upsilon_j(t))=1$ and $\lim D(\Upsilon_i(t),\Upsilon_k(t))=0$. Then, $b_j\approx\frac{1}{e^2}$ and $b_k\approx 0$.

$$\omega_{ij}=\frac{1}{\sum_{k=1,k\neq i}^{N}\frac{1+b_je^{2\eta}}{1+b_ke^{2\eta}}}$$
$$\approx\frac{1}{\sum_{k=1,k\neq i}^{N}(1+\frac{e^{2\eta}}{e^2})}=\frac{1}{(N-1)(1+e^{2(\eta-1)})}$$

Note: On the one hand, as N increases, the weight of the inconsistent agent e_j decreases. When most agents $e_k, k=1,2,\ldots,N, k\neq j$ share the same information, the weight of the only inconsistent agent e_j becomes very small. This helps reduce the negative impact of subjective bias on the final result. Since it is difficult to ensure that all agents provide fully objective information in group decision-making, some level of bias is unavoidable. The proposed method effectively mitigates this problem. On the other hand, the weight ω_{ij} decreases as η increases, meaning that with a larger η, an agent focuses more on information that closely matches its own. When η is smaller, ω_{ij} remains relatively large, so even information with greater differences is still considered.

- Contrary to the above case, $\Upsilon_j(t)$ and $\Upsilon_i(t)$ are the same and the other information $\Upsilon_k(t)$ is pretty different from $\Upsilon_i(t)$, i.e., $D(\Upsilon_i(t),\Upsilon_j(t))=0$ and $\lim D(\Upsilon_i(t),\Upsilon_k(t))=1$. Then, $b_j\approx 0$ and $b_k=\frac{1}{e^2}$ under these conditions it follows that the weights w_{ij} can be expressed as:

$$\omega_{ij}=\frac{1}{\sum_{k=1,k\neq i}^{N}\frac{1+b_je^{2\eta}}{1+b_ke^{2\eta}}}\approx\frac{1}{\sum_{k=1,k\neq i}^{N}\frac{1}{1+\frac{e^{2\eta}}{e^2}}}=\frac{1+e^{2(\eta-1)}}{N-1}$$

Note: As N increases, the weight of the inconsistent agent e_j gradually decreases. This indicates that when the information from other agents differs significantly from $\Upsilon_i(t)$, the weight of the only consistent agent e_j also becomes very low. This further demonstrates that the proposed algorithm can effectively identify inconsistent information and mitigate its negative impact on information evolution by actively reducing its weight. On the other hand, the weight ω_{ij} increases as η increases. When η is large, the weight of e_j also increases, further showing that the proposed algorithm can unify the HK model and the DeGroot model by adjusting the value of η.

Theorem 2: For e_i and e_j, if $\Upsilon_i(t) = \Upsilon_j(t)$, then $\Upsilon_i(t^*) = \Upsilon_j(t^*)$ for all $t^* \geq t$.

Proof :

$$\upsilon_i(t+1) = \sum_{k=1,k\neq i,k\neq j}^{N} \omega_{ik}(t)\upsilon_k(t) + \omega_{ij}(t)\upsilon_j(t)$$

$$\upsilon_j(t+1) = \sum_{k=1,k\neq i,k\neq j}^{N} \omega_{jk}(t)\upsilon_k(t) + \omega_{ji}(t)\upsilon_i(t)$$

Since $\omega_{ij}(t) = \omega_{ji}(t)$ and $\upsilon_i(t) = \upsilon_j(t)$, we can obtain:

$$\upsilon_i(t+1) = \upsilon_j(t+1),\ t^* \geq t$$

and

$$\Upsilon_i(t+1) = \Upsilon_j(t+1),\ t^* \geq t$$

Theorem 3: Assume that there are N agents, χ agents of them have the same information $\Upsilon_i(t) = h_{\xi_1}$. The remaining ψ agents have the information h_{ξ_2}. $\chi + \psi = N$. If $\chi = N-1$ and $\psi = 1$, these N agents will certainly eventually reach the consensus, regardless of whether $h_{\xi_1} = h_{\xi_2}$ or not.

Proof:

1) $h_{\xi_1} = h_{\xi_2}$;

Since $\Upsilon_i(t) = h_{\xi_1}$, $i = 1,2,\cdots,N$, then,

$$\upsilon_i(t+1) = \sum_{j=1}^{N-1} \frac{1}{N-1}\upsilon_j(t) = \theta_{\xi_1}$$

Therefore, $\Upsilon_i(t+1) = h_{\xi_1}$.

2) $h_{\xi_1} \neq h_{\xi_2}$.

• $\theta_{\xi_1} > \theta_{\xi_2}$;

Since

$$\upsilon_j(t+1) = \sum_{i=1,i\neq j}^{N} \frac{1}{N-1}\upsilon_i(t) = \theta_{\xi_1}$$

Hence, $\Upsilon_j(t+1) = h_{\xi_1}$.

Also,

$$\begin{aligned}\upsilon_i(t+1) &= \sum_{k=1,k\neq i}^{N-1} \omega_{ik}(t)\upsilon_k(t) + \omega_{ij}(t)\upsilon_j(t)\\ &= \omega_{i1}(t)\upsilon_1(t) + \cdots + \omega_{i(N-1)}(t)\upsilon_{N-1}(t) + \omega_{ij}(t)\upsilon_j(t)\end{aligned}$$

where $\omega_{i1}(t) = \omega_{i2}(t) = \cdots = \omega_{ik}(t) = \cdots = \omega_{i(N-1)}(t) \neq \omega_{ij}(t)$ and $\upsilon_1(t) = \upsilon_2(t) = \cdots = \upsilon_k(t) = \cdots = \upsilon_{N-1}(t) = \theta_{\xi_1} > \upsilon_j(t)$, $k \neq j$.

Then,

$$\upsilon_i(t+1) = (1-\omega_{ij}(t))\theta_{\xi_1} + \omega_{ij}(t)\theta_{\xi_2}$$

To prove that the system will reach consensus, we need to show that the upper and lower bound distances of this system decrease after one step of iteration. In other words,

$$\max \upsilon_i(t+1) \leq \max \upsilon_k(t),\ i,k = 1,2,\cdots,N$$

$$\min \upsilon_i(t+1) \geq \min \upsilon_k(t),\ i,k = 1,2,\cdots,N$$

It can be obtained that $(1-\omega_{ij}(t))\theta_{\xi_1} + \omega_{ij}(t)\theta_{\xi_2} > \theta_{\xi_2} \rightarrow (1-\omega_{ij}(t))\theta_{\xi_1} > (1-\omega_{ij}(t))\theta_{\xi_2} \rightarrow \theta_{\xi_1} > \theta_{\xi_2}$.

Therefore, $\upsilon_i(t+1) > \upsilon_j(t)$, and we have proven the first iteration.

$$\upsilon_j(t+2) = \upsilon_i(t+1)$$

and

$$\upsilon_i(t+2) = \sum_{k=1,k\neq j}^{N-1} \omega'_{ik}(t+1)\upsilon_k(t+1) + \omega'_{ij}(t+1)\upsilon_j(t+1)$$

where $\omega'_{i1}(t+1) = \omega'_{i2}(t+1) = \cdots = \omega'_{ik}(t+1) = \cdots = \omega'_{i(N-1)}(t+1) \neq \omega'_{ij}(t+1)$ and $\upsilon_1(t+1) = \upsilon_2(t+1) = \cdots = \upsilon_k(t+1) = \cdots = \upsilon_{N-1}(t+1)$.

If these agents gradually reach the consensus, then it must satisfy:

$$\upsilon_i(t+2) < \upsilon_j(t+1)$$

That is

$$\begin{aligned}&\sum_{k=1,k\neq j}^{N-1} \omega'_{ik}(t+1)\upsilon_k(t+1) + \omega'_{ij}(t+1)\upsilon_j(t+1) < \upsilon_j(t+1)\\ &\rightarrow (1-\omega'_{ij}(t+1))\upsilon_i(t+1) + \omega'_{ij}(t+1)\upsilon_j(t+1) < \upsilon_j(t+1)\\ &\rightarrow \upsilon_i(t+1) < \upsilon_j(t+1)\end{aligned}$$

According to the above proof, we know $\upsilon_i(t+1) < \upsilon_j(t+1)$. Therefore, $\upsilon_i(t+2) < \upsilon_j(t+1)$.

The subsequent iterations prove similarly until the agents reach the consensus.

• $\theta_{\xi_1} < \theta_{\xi_2}$;

Based on the above derivation, we can obtain

$$\upsilon_j(t+1) = \theta_{\xi_1}$$

$$\upsilon_i(t+1) = \omega_{i1}(t)\upsilon_1(t) + \cdots + \omega_{i(N-1)}(t)\upsilon_{N-1}(t) + \omega_{ij}(t)\upsilon_j(t)$$

where $\omega_{i1}(t) = \omega_{i2}(t) = \cdots = \omega_{ik}(t) = \cdots = \omega_{i(N-1)}(t) \neq \omega_{ij}(t)$ and $\upsilon_1(t) = \upsilon_2(t) = \cdots = \upsilon_k(t) = \cdots = \upsilon_{N-1}(t)$, $k \neq j$.

Because $\theta_{\xi_1} < \theta_{\xi_2}$, so we need prove $\upsilon_i(t+1) < \upsilon_j(t)$, i.e.,

$$(1-\omega_{ij}(t))\theta_{\xi_1} + \omega_{ij}(t)\theta_{\xi_2} < \theta_{\xi_2}$$

Obviously, the inequality holds. The rest of the proof process is similar to the above and will not be described.

Combining the above proofs we can get that if $\Upsilon_i(t) = h_{\xi_1}$ for $i = 1,2,\cdots,N, i \neq j$ and $\Upsilon_j(t) = h_{\xi_2}$, these agents will certainly eventually reach the consensus, regardless of whether $h_{\xi_1} = h_{\xi_2}$ or not.

Theorem 4: Further study of *Theorem 3*. Whether these N agents can reach the consensus will be largely determined by the number of χ and ψ.

Proof:

According to the above derivation, we can obtain:

$$\upsilon_i(t+1) = \sum_{k=1,k\neq i}^{\chi} \omega_{ik}(t)\upsilon_k(t) + \sum_{q=1}^{\psi} \omega'_{iq}(t)\upsilon_q(t)$$
$$\upsilon_j(t+1) = \sum_{k=1}^{\chi} \omega_{jk}(t)\upsilon_k(t) + \sum_{q=1,q\neq j}^{\psi} \omega'_{jq}(t)\upsilon_q(t)$$

where $\omega_{i1}(t) = \omega_{i2}(t) = \cdots = \omega_{i\chi}(t)$, $\omega'_{i1}(t) = \omega'_{i2}(t) = \cdots = \omega'_{i\psi}(t)$, $\omega_{j1}(t) = \omega_{j2}(t) = \cdots = \omega_{j\chi}(t)$, and $\omega'_{j1}(t) = \omega'_{j2}(t) = \cdots = \omega'_{j\psi}(t)$.

Then, we can derive:

$$\omega_{ik}(t) = \frac{1-\psi\omega'_{iq}(t)}{\chi-1}, \ \ \omega_{jk}(t) = \frac{1-(\psi-1)\omega'_{jq}(t)}{\chi}$$

Therefore,

$$\upsilon_i(t+1) = (1-\psi\omega'_{iq}(t))\theta_{\xi_1} + \psi\omega'_{iq}(t)\theta_{\xi_2}$$
$$\upsilon_j(t+1) = (1-(\psi-1)\omega'_{jq}(t))\theta_{\xi_1} + (\psi-1)\omega'_{jq}(t)\theta_{\xi_2}$$

Here, we divide the discussion into two cases.

- $\theta_{\xi_2} > \theta_{\xi_1}$, i.e., $\upsilon_j(t) > \upsilon_i(t)$;

Based on this prerequisite, we can obtain $\psi\omega'_{iq}(t)\theta_{\xi_2} > \psi\omega'_{iq}(t)\theta_{\xi_1} \to (1-\psi\omega'_{iq}(t))\theta_{\xi_2} < (1-\psi\omega'_{iq}(t))\theta_{\xi_1} \to (1-\psi\omega'_{iq}(t))\theta_{\xi_1} + \psi\omega'_{iq}(t)\theta_{\xi_2} > \theta_{\xi_1} \to \upsilon_i(t+1) > \theta_{\xi_1} = \upsilon_i(t)$.

Given that $\theta_{\xi_2} > \theta_{\xi_1}$ and $(\psi-1)\omega'_{jq}(t)\theta_{\xi_1} < (\psi-1)\omega'_{jq}(t)\theta_{\xi_2}$, then

$$(1-(\psi-1)\omega'_{jq}(t))\theta_{\xi_1} < (1-(\psi-1)\omega'_{jq}(t))\theta_{\xi_2}$$
$$\to (1-(\psi-1)\omega'_{jq}(t))\theta_{\xi_1} + (\psi-1)\omega'_{jq}(t)\theta_{\xi_2} < \theta_{\xi_2}$$

Therefore, $\upsilon_j(t+1) < \upsilon_j(t)$.

- $\theta_{\xi_2} < \theta_{\xi_1}$, i.e., $\upsilon_j(t) < \upsilon_i(t)$;

Based on this prerequisite, we can obtain:

$$\psi\omega'_{iq}(t)\theta_{\xi_2} < \psi\omega'_{iq}(t)\theta_{\xi_1}$$
$$\to (1-\psi\omega'_{iq}(t))\theta_{\xi_2} > (1-\psi\omega'_{iq}(t))\theta_{\xi_1}$$
$$\to (1-\psi\omega'_{iq}(t))\theta_{\xi_1} + \psi\omega'_{iq}(t)\theta_{\xi_2} < \theta_{\xi_1}$$
$$\to \upsilon_i(t+1) < \theta_{\xi_1} = \upsilon_i(t)$$

Similarly, we can obtain $\upsilon_j(t+1) > \upsilon_j(t)$.

To sum up the two cases above, it can be seen that $\upsilon_i(t)$ and $\upsilon_j(t)$ are gradually converging after stepwise iterations. Here, we also need to consider a special case. After iterations, the distance measure $D(\Upsilon_i(t^*), \Upsilon_j(t^*))$ between $\upsilon_i(t^*)$ and $\upsilon_j(t^*)$ is the minimum for $D(\Upsilon_i, \Upsilon_j)$, $i,j = 1,2,\cdots,N$, meanwhile, $\Upsilon_i(t^*) \neq \Upsilon_j(t^*)$. Take the case $\upsilon_i(t^*) < \upsilon_j(t^*)$ as an example.

$$\upsilon_i(t^*+1) = (1-\psi\omega'_{iq}(t^*))\upsilon_i(t^*) + \psi\omega'_{iq}(t^*)\upsilon_j(t^*)$$
$$\upsilon_j(t^*+1) = (1-(\psi-1)\omega'_{jq}(t^*))\upsilon_i(t^*) + (\psi-1)\omega'_{jq}(t^*)\upsilon_j(t^*)$$

If χ is very large, even $N-1$ or $N-2$, then $\psi\omega'_{iq}(t^*)$ is very small and $\psi\omega'_{iq}(t^*)\upsilon_j(t^*)$ is close to 0. $\upsilon_i(t^*+1)$ most likely belongs to the interval $(\upsilon_i(t^*), (\upsilon_i(t^*) + \upsilon_{i,\xi(1)}(t^*))/2)$ and $\upsilon_i(t^*+1) \approx \upsilon_i(t^*)$. For $\upsilon_j(t^*+1)$, $(\psi-1)\omega'_{jq}(t^*)$ is very small and $(\psi-1)\omega'_{jq}(t^*)\upsilon_j(t^*)$ is close to 0. Then, $\upsilon_j(t^*+1) \approx \upsilon_i(t^*)$. The agents reach the consensus.

On the other hand, if χ and ψ are close, like $\chi = \psi = \frac{N}{2}$, then, $1-\psi\omega'_{iq}(t^*)$ and $\psi\omega'_{iq}(t^*)$ may not be significantly different. Also, $(1-(\psi-1)\omega'_{jq}(t^*))$ and $(\psi-1)\omega'_{jq}(t^*)$ are not very different. In this case, it is not easy to determine that $\Upsilon_i(t^*+1))$ and $\Upsilon_j(t^*+1))$ are $\Upsilon_i(t^*)$ or $\Upsilon_j(t^*)$. Therefore, if the opinions of χ agents are the same, all of them are $\Upsilon_i(t) = h_{\xi_1}$, $i = 1,2,\cdots,\chi$. The information of remaining ψ agents is $\Upsilon_j(t) = h_{\xi_2}$, $j = 1,2,\cdots,\psi$, $\chi+\psi = N$. Then, whether these N agents can reach the consensus will be largely determined by the number of χ and ψ.

Theorem 5: Further study of *Theorem 4*. The agents will reach the consensus as long as $|\upsilon_j(t+1) - \upsilon_i(t+1)|$ is less than a very small value for all agents. The ideal state is $(\chi-1)(\psi-1) = g^2(\frac{1}{D(h_{\xi_1},h_{\xi_2})})\chi\psi$.

Proof :

Let $\alpha = (\chi-1) + g\Big(\frac{1}{D(h_{\xi_1},h_{\xi_2})}\Big)\psi$ and $\beta = (\psi-1) + g\Big(\frac{1}{D(h_{\xi_1},h_{\xi_2})}\Big)\chi$, then $\upsilon_i(t+1) = \frac{\chi-1}{\alpha}\upsilon_i(t) + \Big(1-\frac{\chi-1}{\alpha}\Big)\upsilon_j(t)$ and $\upsilon_j(t+1) = \Big(1-\frac{\psi-1}{\beta}\Big)\upsilon_i(t) + \frac{\psi-1}{\beta}\upsilon_j(t)$.

Then,

$$\begin{aligned}\upsilon_j(t+1) - \upsilon_i(t+1) = \\ &\bigg(\Big(1-\frac{\psi-1}{\beta}\Big)\upsilon_i(t) + \frac{\psi-1}{\beta}\upsilon_j(t)\bigg) \\ &-\bigg(\frac{\chi-1}{\alpha}\upsilon_i(t) + \Big(1-\frac{\chi-1}{\alpha}\Big)\upsilon_j(t)\bigg) \\ &= \bigg(1-\frac{\psi-1}{\beta}-\frac{\chi-1}{\alpha}\bigg)\Big(\upsilon_i(t)-\upsilon_j(t)\Big)\end{aligned}$$

Since $\upsilon_i(t) \neq \upsilon_j(t)$, for $\upsilon_j(t+1) = \upsilon_i(t+1)$, the ideal state is $1-\frac{\psi-1}{\beta}-\frac{\chi-1}{\alpha} = 0$, i.e., $\bigg((\chi-1) + g\Big(\frac{1}{D(h_{\xi_1},h_{\xi_2})}\Big)\psi\bigg)(\psi-1) + \bigg((\psi-1) + g\Big(\frac{1}{D(h_{\xi_1},h_{\xi_2})}\Big)\chi\bigg)(\chi-1) = \bigg((\chi-1) + g\Big(\frac{1}{D(h_{\xi_1},h_{\xi_2})}\Big)\psi\bigg) \cdot \bigg((\psi-1) + g\Big(\frac{1}{D(h_{\xi_1},h_{\xi_2})}\Big)\chi\bigg)$.

Then,

$$\begin{aligned}&2(\chi-1)(\psi-1) + g\Big(\frac{1}{D(h_{\xi_1},\, h_{\xi_2})}\Big)\Big(\chi(\chi-1)+\psi(\psi-1)\Big) \\ &= (\chi-1)(\psi-1) + g\Big(\frac{1}{D(h_{\xi_1},\, h_{\xi_2})}\Big)\Big(\chi(\chi-1)+\psi(\psi-1)\Big) \\ &+ g^2\Big(\frac{1}{D(h_{\xi_1},\, h_{\xi_2})}\Big)\chi\psi.\end{aligned}$$

Therefore, $(\chi-1)(\psi-1) = g^2(\frac{1}{D(h_{\xi_1},h_{\xi_2})})\chi\psi$.

References

[1] H. Liu, Y. Yu, S. Liu, and W. Wang, "A military object detection model of uav reconnaissance image and feature visualization," *Applied Sciences*, vol. 12, no. 23, p. 12236, 2022.

[2] W. Jin, J. Yang, Y. Fang, and W. Feng, "Research on application and deployment of uav in emergency response," in *2020 IEEE 10th international conference on electronics information and emergency communication (ICEIEC)*. IEEE, 2020, pp. 277–280.

[3] Y. Wang, Z. Su, Q. Xu, R. Li, T. H. Luan, and P. Wang, "A secure and intelligent data sharing scheme for uav-assisted disaster rescue," *IEEE/ACM Transactions on Networking*, vol. 31, no. 6, pp. 2422–2438, 2023.

[4] H. Liu, Y. P. Tsang, C. K. Lee, and C. H. Wu, "Uav trajectory planning via viewpoint resampling for autonomous remote inspection of industrial facilities," *IEEE Transactions on Industrial Informatics*, 2024.

[5] K. Liu and B. M. Chen, "Industrial uav-based unsupervised domain adaptive crack recognitions: From database towards real-site infrastructural inspections," *IEEE Transactions on Industrial Electronics*, vol. 70, no. 9, pp. 9410–9420, 2022.

[6] Y. Wang, Z. Su, Q. Xu, R. Li, and T. H. Luan, "Lifesaving with rescuechain: Energy-efficient and partition-tolerant blockchain based secure information sharing for uav-aided disaster rescue," in *IEEE INFOCOM 2021-IEEE Conference on Computer Communications*. IEEE, 2021, pp. 1–10.

[7] X. Fu and T. Chen, "Supply chain network optimization based on fuzzy multiobjective centralized decision-making model," *Mathematical Problems in Engineering*, vol. 2017, no. 1, p. 5825912, 2017.

[8] Z. Liu, Y. Li, and Y. Wu, "Multiple uav formations delivery task planning based on a distributed adaptive algorithm," *Journal of the Franklin Institute*, vol. 360, no. 4, pp. 3047–3076, 2023.

[9] D. Liu, Q. Zong, X. Zhang, R. Zhang, L. Dou, and B. Tian, "Game of drones: Intelligent online decision making of multi-uav confrontation," *IEEE Transactions on Emerging Topics in Computational Intelligence*, vol. 8, no. 2, pp. 2086–2100, 2024.

[10] J. Wang, Y. Hong, J. Wang, J. Xu, Y. Tang, Q.-L. Han, and J. Kurths, "Cooperative and competitive multi-agent systems: From optimization to games," *IEEE/CAA Journal of Automatica Sinica*, vol. 9, no. 5, pp. 763–783, 2022.

[11] F. Seredyński, T. Kulpa, and R. Hoffmann, "Towards evolutionary self-optimization of large multi-agent systems," in *Proceedings of the Genetic and Evolutionary Computation Conference Companion*, 2022, pp. 200–203.

[12] Y. Dong, X. Liu, T. Li, and C. P. Chen, "Evolutionary game dynamics of multi-agent systems using local information considering hide right," *Complex & Intelligent Systems*, vol. 10, no. 1, pp. 917–925, 2024.

[13] W. Yu, Z. Zhang, and Q. Zhong, "Consensus reaching for magdm with multi-granular hesitant fuzzy linguistic term sets: a minimum adjustment-based approach," *Annals of Operations Research*, vol. 300, no. 2, pp. 443–466, 2021.

[14] M. Bi, D. M. Tilbury, S. Shen, and K. Barton, "A distributed approach for agile supply chain decision-making based on network attributes," *IEEE Transactions on Automation Science and Engineering*, vol. 21, no. 3, pp. 2223–2236, 2023.

[15] M. Brittain and P. Wei, "Scalable autonomous separation assurance with heterogeneous multi-agent reinforcement learning," *IEEE Transactions on automation science and engineering*, vol. 19, no. 4, pp. 2837–2848, 2022.

[16] P. Li, Z. Xu, Z. Zhang, Z. Li, and C. Wei, "Consensus reaching in multi-criteria social network group decision making: A stochastic multicriteria acceptability analysis-based method," *Information Fusion*, vol. 97, p. 101825, 2023.

[17] X. Chen, Z. Ding, Y. Gao, H. Zhang, and Y. Dong, "Competitive resource allocation on a network considering opinion dynamics with self-confidence evolution," *Information Fusion*, vol. 114, p. 102680, 2025.

[18] X. Chen, Z. Ding, Y. Dong, and H. Liang, "Managing consensus with minimum adjustments in group decision making with opinions evolution," *IEEE Transactions on Systems, Man, and Cybernetics: Systems*, vol. 51, no. 4, pp. 2299–2311, 2019.

[19] Z. Wu, Q. Zhou, Y. Dong, J. Xu, A. H. Altalhi, and F. Herrera, "Mixed opinion dynamics based on degroot model and hegselmann–krause model in social networks," *IEEE Transactions on Systems, Man, and Cybernetics: Systems*, vol. 53, no. 1, pp. 296–308, 2022.

[20] Q. Liang, C. Luo, Z. Zhang, and D. Cheng, "Mining maximum ordinal-cardinal consensus for large-scale group decision making with incomplete fuzzy preference relations," *IEEE Transactions on Fuzzy Systems*, 2024.

[21] Z. Zhang and Z. Li, "Personalized individual semantics-based consistency control and consensus reaching in linguistic group decision making," *IEEE Transactions on Systems, Man, and Cybernetics: Systems*, vol. 52, no. 9, pp. 5623–5635, 2021.

[22] F. Pei, Y. Gao, A. Yan, M. Zhou, and J. Wu, "Conflict elimination based on opinion dynamics in fuzzy group decision-making," *Expert Systems with Applications*, p. 124308, 2024.

[23] Z. Wu, Q. Zhou, Y. Dong, J. Xu, A. H. Altalhi, and F. Herrera, "Mixed opinion dynamics based on degroot model and hegselmann–krause model in social networks," *IEEE Transactions on Systems, Man, and Cybernetics: Systems*, vol. 53, no. 1, pp. 296–308, 2023.

[24] Y. Li, M. Liu, J. Cao, X. Wang, and N. Zhang, "Multi-attribute group decision-making considering opinion dynamics," *Expert Systems with Applications*, vol. 184, p. 115479, 2021.

[25] H. Liang, C.-C. Li, Y. Dong, and F. Herrera, "Linguistic opinions dynamics based on personalized individual semantics," *IEEE Transactions on Fuzzy Systems*, vol. 29, no. 9, pp. 2453–2466, 2021.

[26] J. Wu, Z. Zhao, Q. Sun, and H. Fujita, "A maximum self-esteem degree based feedback mechanism for group consensus reaching with the distributed linguistic trust propagation in social network," *Information Fusion*, vol. 67, pp. 80–93, 2021.

[27] F. Jin, J. Liu, L. Zhou, and L. Martínez, "Consensus-based linguistic distribution large-scale group decision making using statistical inference and regret theory," *Group Decision and Negotiation*, vol. 30, no. 4, pp. 813–845, 2021.

[28] Y. Liu, L. Zhu, R. M. Rodríguez, Y. Yao, and L. Martínez, "Three-way group decision-making with personalized numerical scale of comparative linguistic expression: An application to traditional chinese medicine," *IEEE Transactions on Fuzzy Systems*, vol. 32, no. 8, pp. 4352–4363, 2024.

[29] Z. Zhang, W. Yu, L. Martínez, and Y. Gao, "Managing multigranular unbalanced hesitant fuzzy linguistic information in multiattribute large-scale group decision making: A linguistic distribution-based approach," *IEEE Transactions on Fuzzy Systems*, vol. 28, no. 11, pp. 2875–2889, 2020.

[30] C.-C. Li, H. Liang, Y. Dong, F. Chiclana, and E. Herrera-Viedma, "Consistency improvement with a feedback recommendation in personalized linguistic group decision making," *IEEE Transactions on Cybernetics*, pp. 1–12, 2021.

[31] L. A. Zadeh, "The concept of a linguistic variable and its application to approximate reasoning," *Information Sciences*, vol. 8, no. 3, pp. 199–249, 1974.

[32] G. Y. Bao, X. L. Lian, M. He, and L. L. Wang, "Improved two-tuple linguistic representation model based on new linguistic evaluation scale," *Control & Decision*, vol. 25, no. 5, pp. 780–784, 2010.

[33] Y. Dong, Z. Ding, L. Martínez, and F. Herrera, "Managing consensus based on leadership in opinion dynamics," *Information Sciences*, vol. 397, pp. 187–205, 2017.

[34] J. Wu and F. Chiclana, "A social network analysis trust–consensus based approach to group decision-making problems with interval-valued fuzzy reciprocal preference relations," *Knowledge-Based Systems*, vol. 59, pp. 97–107, 2014.

[35] J. Wu, M. Cao, F. Chiclana, Y. Dong, and E. Herrera-Viedma, "An optimal feedback model to prevent manipulation behavior in consensus under social network group decision making," *IEEE Transactions on Fuzzy Systems*, vol. 29, no. 7, pp. 1750–1763, 2021.

[36] Q. Jia and E. Herrera-Viedma, "3-d golden rule representative value in decision-making systems," *IEEE Transactions on Fuzzy Systems*, vol. 32, no. 6, pp. 3729–3740, 2024.

[37] A. W. Wolfe, "Social network analysis: Methods and applications," *Contemporary Sociology*, vol. 91, no. 435, pp. 219–220, 1995.

[38] R.-X. Ding, X. Wang, K. Shang, and F. Herrera, "Social network analysis-based conflict relationship investigation and conflict degree-based consensus reaching process for large scale decision making using sparse representation," *Information Fusion*, vol. 50, pp. 251–272, 2019.

[39] S. Huang, J. Shi, Q. Zhu, Z. Du, Y. Lyu, and Z. Liu, "Multiple uavs cooperatively circumnavigating a group of non-cooperative targets in a gps-free environment via a range-only distributed controller," *Aerospace Science and Technology*, vol. 158, p. 109924, 2025.